STATE RESEARCH CENTER OF RUSSIA
INSTITUTE FOR HIGH ENERGY PHYSICS

IHEP 2008-21

Yu.V.Kharlov, P.A.Semenov, Yu.A.Matulenko, O.P.Yushchenko,
Yu.I.Arestov, G.I.Britvich, S.K.Chernichenko, Yu.M.Goncharenko,
A.M.Davidenko, A.A.Derevschikov, A.S.Konstantinov, V.A.Kormilitsyn,
V.I.Kravtsov, Yu.M.Melnik, A.P.Meschanin, N.G.Minaev, V.V.Mochalov,
D.A.Morozov, A.V.Ryazantsev, I.V.Shein, A.P.Soldatov, L.F.Soloviev,
A.V.Soukhikh, A.N.Vasiliev, M.N.Ukhanov, V.G.Vasilchenko, A.E.Yakutin

PERFORMANCE OF A FINE-SAMPLING ELECTROMAGNETIC CALORIMETER PROTOTYPE IN THE ENERGY RANGE FROM 1 TO 19 GEV

Submitted to *Nucl. Instrum. Meth. A*

Protvino 2008

UDK 539.1.074 M–24

Abstract

Kharlov Yu.V., Semenov P.A., Matulenko Yu.A. et al. Performance of a Fine-Sampling Electromagnetic Calorimeter Prototype in the Energy Range from 1 to 19 GeV: IHEP Preprint 2008-21. – Protvino, 2008. – p. 11, figs. 9, tables 3, refs.: 15.

The fine-sampling electromagnetic calorimeter prototype has been experimentally tested using the 1–19 GeV/c tagged beams of negatively charged particles at the U70 accelerator at IHEP, Protvino. The energy resolution measured by electrons is $\Delta E/E = 2.8\%/\sqrt{E} \oplus 1.3\%$. The position resolution for electrons is $\Delta x = 3.1 \oplus 15.4/\sqrt{E}$ mm in the center of the cell. The lateral non-uniformity of the prototype energy response to electrons and MIPs has turned out to be negligible. Obtained experimental results are in a good agreement with Monte-Carlo simulations.

Аннотация

Харлов Ю.В., Семенов П.А., Матуленко Ю.А. и др. Свойства прототипа электромагнитного калориметра с тонким сэмплингом при энергиях от 1 до 10 ГэВ: Препринт ИФВЭ 2008-21. – Протвино, 2008. – 11 с., 9 рис., 3 табл., библиогр.: 15.

Прототип электромагнитного калориметра с тонким сэмплингом был экспериментально изучен с помошью меченого пучка отрицательно заряженных частиц с импульсом 1–19 ГэВ/с на ускорителе У-70 в ИФВЭ. Измеренное энергетическое разрешение составило $\Delta E/E = 2.8\%/\sqrt{E} \oplus 1.3\%$. Координатное разрешение для электронов составило $\Delta x = 3.1 \oplus 15.4/\sqrt{E}$ мм в центре ячейки. Поперечная неоднородность энергетического отклика прототипа на минимально ионизирующую частицу оказалась незначительной. Полученные экспериментальные результаты находятся в хорошем согласии с Монте–Карло моделированием.

Introduction

Electromagnetic calorimeters are based on the total energy deposition of photons and electrons in the active medium of detectors. Energy deposited by secondary particles of an electromagnetic shower is detected either as a Cherenkov radiation of electrons and positrons, like in the lead-glass calorimeters [1], or as a scintillation light emitted by the active medium [2]. Sampling calorimeters constructed from alternating layers of organic scintillator and heavy absorber, have been used in high energy physics over last tens of years [3]. The sampling of such calorimeters is determined by the required lateral size of electromagnetic shower, expressed by a Molière radius R_M, and the light yield provided by scintillator plates. Scintillation light is absorbed, re-emitted and transported to a photodetector by wave-length shifting (WLS) optical fibers penetrating through the calorimeter modules longitudinally (along the beam direction). Typical stochastic term of the energy resolution of all large electromagnetic calorimeters of the sampling type was about 10% [4, 5, 6].

Recently the improved electromagnetic calorimeter modules with a very fine sampling have been developed for KOPIO experiment at BNL [7]. The energy resolution of these modules, measured with photons of energy 220–350 MeV, was about $3\%/\sqrt{E\ (\mathrm{GeV})}$ [8]. Details of the improved modules tested in the energy range of 50–1000 MeV, including mechanical construction, selection of WLS fibers and photodetectors as well as development of a new scintillator with improved optical and mechanical properties are described in [9].

Similar high-performance electromagnetic calorimeters are now being considered for PANDA and CBM experiments [10,11] at the future FAIR facility, which is under construction at GSI, Darmstadt in Germany. The both fixed target experimental setups require an ability to measure single photons, π^0's as well as η's in the wide energy range with excellent energy and position resolutions. Fine-sampling calorimeters, not very expensive and meanwhile covering wide areas like 3 m^2 in PANDA and 100 m^2 in CBM, were chosen to meet the requirements. The energy range in PANDA and CBM experiments will be extended up to 15 and 35 GeV, respectively. It is essential for these projects to study parameters of a fine-sampling calorimeter in the wide energy region, significantly wider than the one with the existing data (only up to 1 GeV).

In this paper, we describe a fine-sampling electromagnetic calorimeter prototype with lead absorber plates, which thickness is significantly smaller than radiation length X_0 of lead. Such a small thickness of the absorber layers results in a small interaction probability of the secondary

shower particles. The design of this prototype is close to the KOPIO one including the same lateral size of cells. The results of miscellaneous studies of the prototype in the energy range from 1 to 19 GeV are presented in this paper.

1. Design of the modules

The electromagnetic calorimeter modules with fine sampling were constructed at IHEP, Protvino. A module design was based on the electromagnetic calorimeter for the KOPIO experiment, with additional modification to high-energy range. Details of the mechanical design of the modules can be found in [9], but a few modifications were applied to the prototype under study. The KOPIO experiment was aimed to low-energy photons, and the total radiation length $16X_0$ was enough for their purposes. The current prototype is being proposed for CBM and PANDA, where the photon energy extends up to 30 GeV, and the requirement to provide the total radiation length of $20X_0$ was put to the design. The modules were assembled from 380 alternating layers of lead and scintillator plates. Lead plates were doped by 3% of antimony to improve their rigidity. Scintillator plates were made of polystyrene doped by 1.5% of paraterphenile and 0.04% of POPOP. Scintillator was manufactured at the scintillator workshop of IHEP with the use of molding technology. The physical properties of the modules are presented in Table 1.

Lead plate thickness	0.275 mm
Scintillator plate thickness	1.5 mm
Number of layers	380
Effective radiation length, X_0	34 mm
Total radiation length	$20X_0$
Effective Moliere radius, R_M	59 mm
Module size	$110 \times 110 \times 675$ mm^3
Module weight	18 kg

Table 1. Physical properties of the module.

The WLS optical fibers BCF-91A with a diameter of 1.2 mm were used in the modules. Each fiber penetrated through the module along its longitudinal axis twice, forming a loop at the face end of the module. Radius of the loop was 28 mm. In total 72 such looped fibers formed a grid of 12× 12 fibers per module with spacing of 9.3 mm. All 144 fiber ends were assembled into a bundle of a diameter about 10 mm, glued, cut, polished and attached to the photodetector at the downstream end of the module. No optical grease was used to provide an optical contact between the bundle cap and the photodetector, thus there was a natural air gap between them.

A photomutiplier Hamamatsu R5800 was used as a photodetector for the prototype. The diameter of the photocathode is 25.4 mm, the number of dynodes is 10, the applied high voltage was about 1100 V. Each photomultiplier was monitored by LED light guided to the photocathodes by a clear polystyrene fiber.

2. Experimental setup for the prototype studies

The prototype of electromagnetic calorimeter consisted of 9 modules assembled into 3×3 matrix installed on the remotely controlled x, y-moving support positioned the prototype across

the beam with a precision of 0.4 mm. The beam line 2B of the U-70 accelerator was used to study performance of the calorimeter prototype. The secondary beam of negatively charged particles of momenta from 1 to 19 GeV/c contained more than 70% of electrons mixed with muons and hadrons (mainly π^- and K^-). Particle identification was not available at this beam line. A momentum spread of the beam was at the level of 1 to 5% at energies from 45 to 1 GeV, respectively. However, the momentum tagging system[12] gave a beam momentum resolution from 0.13 to 2% in the same momentum range. The tagging system illustrated in Fig. 1 consisted of the dipole magnet `M` and 4 sets of 2-coordinate drift chambers `DC1`–`DC4`. A bending angle of the magnet was 55 mrad.

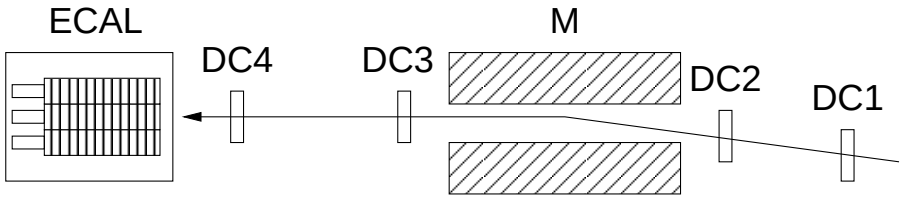

Figure 1. Beam tagging system for the calorimeter prototype studies.

A trigger of the experimental setup used the coincidence of scintillator counters `S1`, `S2` and `S3` installed upstream before the first drift chamber `DC1`, and a scintillator counter `S4` installed after the last drift chamber `DC4` in front of the calorimeter prototype `ECAL`.

An amplitude out of each prototype cell was measured by the 15-bit charge sensitive ADC modules LRS2285 over 150-ns gate with a sensitivity of 30 fC/count. To read out time information from the drift chamber stations TDC, the LRS3377 CAMAC modules were used. Data acquisition system included a couple of crates with ADC and TDC modules as well as control modules to synchronize a read-out process. VME crate with CAMAC parallel branch driver and PCI-VME bridge linked all the electronics into the complete system. Detailed description of the data acquisition system and front-end electronics can be found in [13].

3. Monte-Carlo simulations

The relevant simulation tools were developed. These tools, at the first stage, are intended mainly for cross-check of experimental results as well as for tuning of the reconstruction algorithms.

Having proved the consistency of Monte-Carlo and the real data, we plan to use these tools for further optimization of module design and reconstruction algorithms to provide better performance of the photons and π^0's reconstruction. Simulation studies were performed with GEANT3 as a Monte-Carlo engine with detailed description of materials and module geometry.

The developing shower produces light which originates from two different sources:

- scintillation in plastic plates due to continuous energy losses when charged particles pass through the active calorimeter material,
- Cherenkov radiation when charged particles pass through the WLS fibers.

The simplified technique consists of counting energy deposition in the active material (with some corrections to take into account light attenuation in the fibers) and ignoring Cherenkov radiation

inside the fibers. This method is very fast while can not reproduce all details of the calorimeter response such as non-uniformity due to fibers and cell borders.

For these studies, the detailed light propagation was applied taking into account the optical properties of the materials, internal reflections at plate borders, light capture by fibers with double cladding and the Cherenkov light production and propagation inside the fibers. It was assumed that attenuation length was 70 cm in the scintillator and 400 cm in the fiber, scintillator refraction index is 1.59, total internal reflection efficiency at large scintillator faces is 0.97 and reflection of diffusion type was assumed at side scintillator faces with the same probability. The mean deposited energy for one optical photon production in the scintillator was assumed to be 100 eV and the Cherenkov photons were generated by GEANT.

4. Results

4.1. Calibration of the modules

The modules were calibrated by a 19-GeV/c beam. Each module was exposed to the beam using an x, y-moving support. The energy spectrum from one module (Fig. 2, left plot) shows a peak at 19 GeV corresponding to the energy deposited by electrons. Another peak at low energies is due to minimum ionizing particles (MIP). A broad distribution in the energy specrtum between the two peaks is due to hadrons. Calibration of the modules was possible using both electron and MIP signals, but the best relative calibration coefficients were found by equalizing MIP signals, while the absolute calibration was obtained by setting the total measured energy in the 3×3 matrix to 19 GeV. Events when only one module has an energy above the threshold of 100 MeV were selected for the MIP calibration.

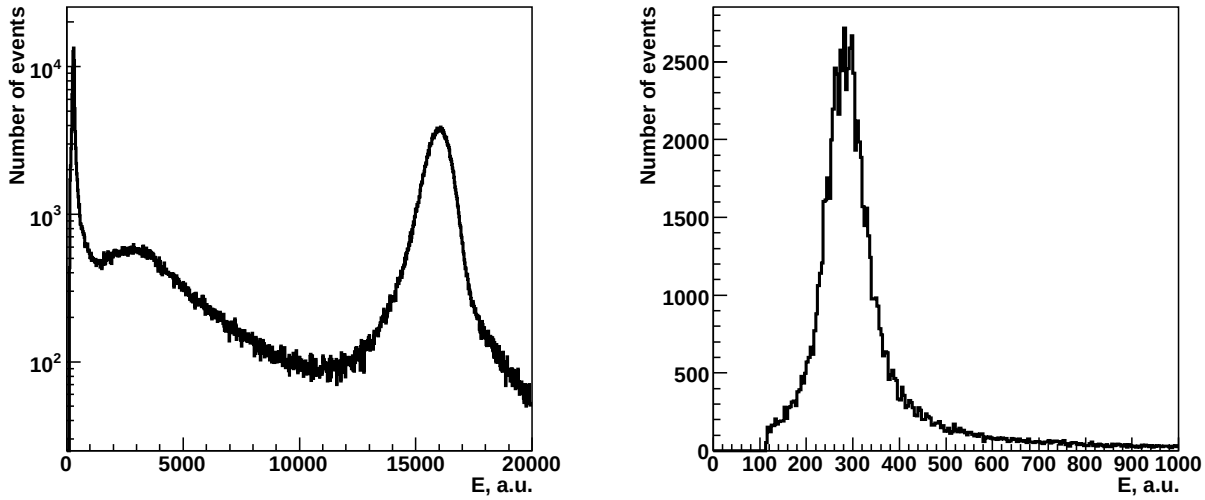

Figure 2. Energy deposited by the 19-GeV/c beam in one module.

The energy distribution around the MIP peak (Fig. 2, right plot) has two contributions. One is caused by the Landau distribution of ionization energy loss, and another one is due to the finite energy resolution of the calorimeter at low energy. The MIP peak was fitted by the Gaussian, and the mean value of the fitting function served for the relative calibration.

4.2. Energy and position resolution

After some dedicated calibration runs, when each module was exposed to the 19-GeV/c beam, the ECAL prototype was fixed so that the beam hit the central module. It was exposed to beam at momenta 1; 2; 3.5; 5; 7; 10, 14 and 19 GeV/c. For each beam momentum, magnetic field in the spectrometric magnet `M` was adjusted to provide the same bending angle of the beam. The momentum of the beam particle p was measured by the magnetic spectrometer, and the energy E measured in the calorimeter prototype is linearly correlated with the momentum p, as illustrated by Fig. 3.

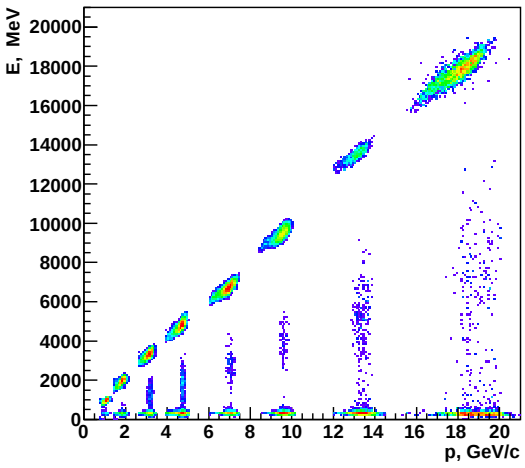

Figure 3. Correlation between the energy measured in the calorimeter and the beam momentum measured in the magnetic spectrometer.

Therefore, in order to obtain a true energy resolution, the measured energy should be corrected by the beam momentum, or the energy resolution can be represented by the width of the distribution of the E/p ratio (Fig. 4).

The energy resolution is obtained from the Gaussian fit of the right peak around $E/p = 1$. The energy resolution $\Delta E/E$ measured by electrons at energies from 1 to 19 GeV are shown in Fig. 5.

The black bullets represent the experimentally measured points. The solid curve is a result of a fit of these experimental points, and the dashed curve is a result of a fit of the Monte-Carlo points. The fitting function can be represented by the equation (1):

$$\frac{\Delta E}{E} = \sqrt{\left(\frac{a}{E}\right)^2 + \frac{b^2}{E} + c^2}, \tag{1}$$

where parameters a, b and c for the experimental and Monte Carlo fits are shown in Table 2.

	a, 10^{-2} GeV	b, 10^{-2} GeV$^{1/2}$	c, 10^{-2}
Experimental fit	3.51 ± 0.28	2.83 ± 0.22	1.30 ± 0.04
Monte Carlo fit	3.33 ± 0.12	3.07 ± 0.08	1.24 ± 0.02

Table 2. Fitting function parameters for the energy resolution.

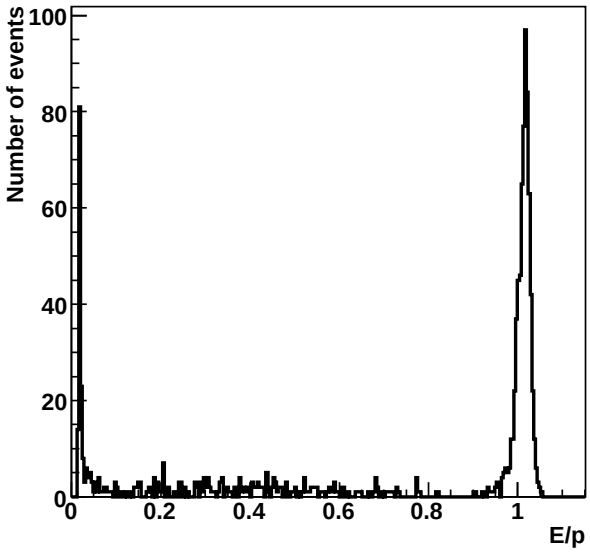

Figure 4. Ratio of the energy E measured in the calorimeter to the momentum p measured by the magnetic spectrometer at 19 GeV/c.

A linear term a of the energy resolution expansion is determined by a beam spread rather than the calorimeter properties. As it was shown in previous studies performed at this 2B beam channel [13], the main contribution to this term comes from the electronics noise and the multiple scattering of the beam particles on the beam pipe flanges and the drift chambers. The beam momentum spread was introduced into Monte-Carlo simulations in order to fully reproduce the experimental conditions. A simulated energy resolution is shown by the red dashed line in Fig. 5.

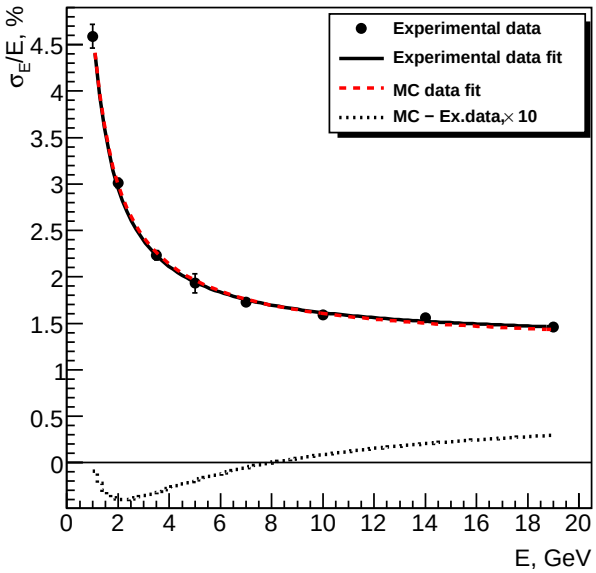

Figure 5. Measured energy resolution.

The dotted line at this plot is a difference between the experimental data fit and the Monte-Carlo fit multiplied by 10. Thus a deviation of the experimental result from the simulation one is less than 0.04%. The energy resolution obtained in Monte-Carlo is in a good agreement with the experimental data. Position resolution has been determined by a comparison of the exact impact coordinate of the beam particle, measured by the last drift chamber DC4, and the center-of-gravity of electromagnetic shower developed in the calorimeter prototype. Fig. 6 shows a dependence of the measured coordinate $x_{\rm rec}$ on the true one x_0.

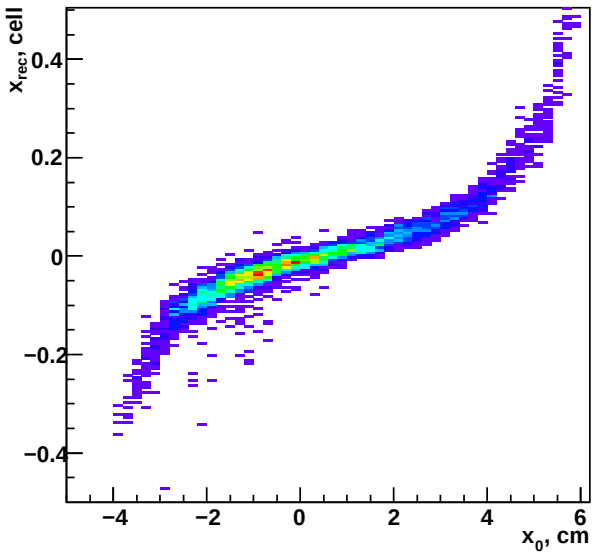

Figure 6. Center of gravity of the electromagnetic shower $X_{\rm rec}$ vs the impact coordinate of the electron x_0.

A position resolution in the middle of the module is shown in Fig. 7, where the bullets represent the experimentally measured points, the solid curve is a result of the experimental points fit, and and the red dashed curve is a result of Monte-Carlo points fit.

The data were fitted by the function (2)

$$\Delta x = \sqrt{a^2 + \frac{b^2}{E}}, \tag{2}$$

where parameters a and b are given in Table 3.

	a, mm	b, mm $\mathrm{GeV}^{1/2}$
Experimental fit	3.09 ± 0.16	15.4 ± 0.3
Monte Carlo fit	3.40 ± 0.14	14.5 ± 0.3

Table 3. Fitting function parameters for the position resolution.

The dotted curve in Fig. 7 stands for a deviation of the experimental data fit results from the Monte-Carlo fit results, which are consistent within 5% of precision.

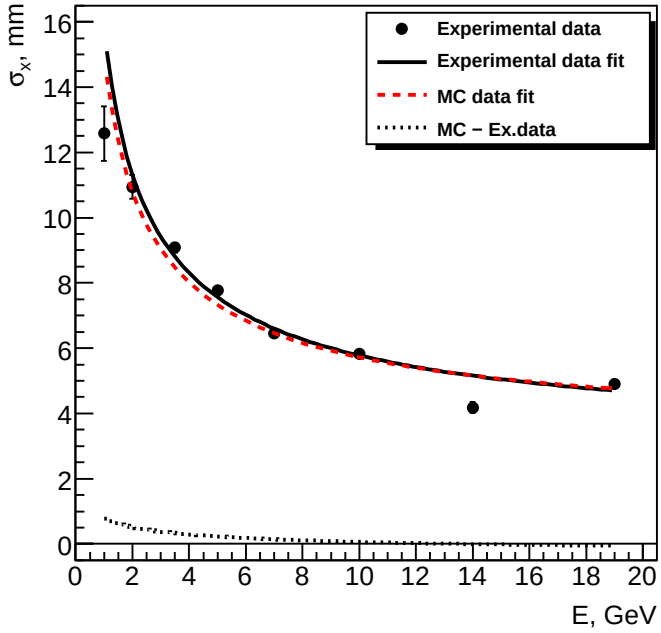

Figure 7. Measured position resolution.

4.3. Lateral non-uniformity

Due to various mechanical inhomogeneities of the prototype one can expect to observe the dependence of the energy E deposited in the calorimeter on the hit coordinates (x, y). The "hot" zones, if any, should be seen at the WLS fiber positions, at the steel strings, and at the boundaries between the modules. A possible lateral non-uniformity of the energy response was studied with the data collected in the 19-GeV/c-run. The last drift chamber `DC4` was used to measure the coordinate of the beam particle incidence onto the calorimeter surface. As the beam contained several particle species which interact differently with the calorimeter medium (see Fig. 2), the mean deposited energy was measured as a function of (x, y) for two energy intervals, $E < 0.5$ GeV and $16 < E < 22$ GeV corresponding to the MIP peak and that of the electromagnetic shower, respectively.

The relative energy response profile for electrons vs y-coordinate at fixed x is shown in Fig. 8. As one can see, the fluctuations of the energy response do not exceed 1%, that is no lateral non-uniformity of the energy response is observed within the available statistics.

4.4. Light output measurement

Light output of the prototype modules, expressed as a number of photoelectrons $N_{\text{p.e.}}$, was evaluated with the highly stable LED pulses [14]. Fluctuations of the measured amplitude A is determined by statistical fluctuations of the number of detected photoelectrons and by fluctuations of the photomultiplier gain M [15]:

$$\left(\frac{\sigma_A}{A}\right)^2 = \frac{1}{N_{\text{p.e.}}}\left[1 + \left(\frac{\sigma_M}{M}\right)^2\right]. \qquad (3)$$

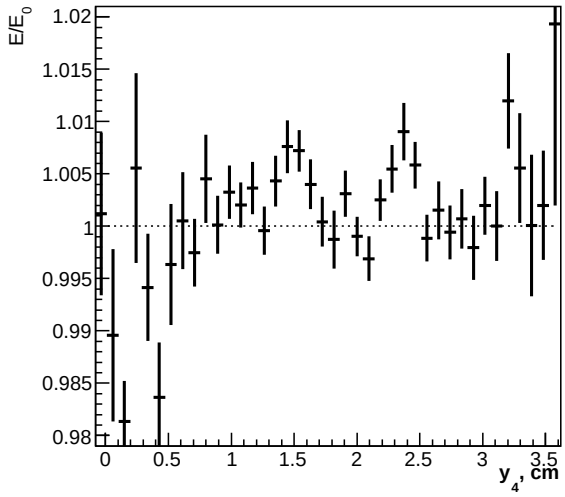

Figure 8. Relative energy response profile vs y-coordinate at fixed x.

The gain fluctuation can be defined through the secondary emission factor of the first dynode δ_1 and the secondary emission factor of other dynodes δ:

$$\left(\frac{\sigma_M}{M}\right)^2 = \frac{\delta}{\delta_1} \cdot \frac{1}{\delta - 1}. \tag{4}$$

The total gain of the 10-dynode photomultiplier R5800 was equal to 10^6 for the applied high voltage 1100 V, and the potential of the first dynode was boosted to increase the secondary emission factor δ_1 to approximately 5. Thus, one can obtain the emission factor $\delta = 3.9$ and the equation (3) is derived to the number of the detected photoelectrons as a function of the relative amplitude width:

$$N_{\text{p.e.}} \approx \frac{1.3}{(\sigma_A/A)^2}. \tag{5}$$

A set of runs with six different LED amplitudes has been carries out. A dependence of the number of photoelectrons on the LED amplitude for one cell and a distribution of the light output for all 9 cells are shown in Fig. 9.

These plots were fitted by the linear function, which slope represents the number of photoelectrons per one ADC count. Being divided by the calibration coefficient, one can obtain that the number of photoelectrons detected by the the prototype modules is (4.8 ± 0.6) p.e./MeV.

Conclusion

The measurements of energy and position resolutions of the electromagnetic calorimeter prototype of fine-sampling type for the PANDA and CBM experiments at FAIR at Darmstadt have been carried out at the IHEP test beam facility at the Protvino 70 GeV accelerator. The prototype consisted of a 3×3 array with the cell sizes of 11×11 cm^2. Each cell had 380 layers with 1.5 mm scintillator and 0.3 mm lead. Scintillation light was collected by optical fibers penetrating through the modules longitudinally along the beam direction. The prototype was designed and assembled at the IHEP scintillator workshop.

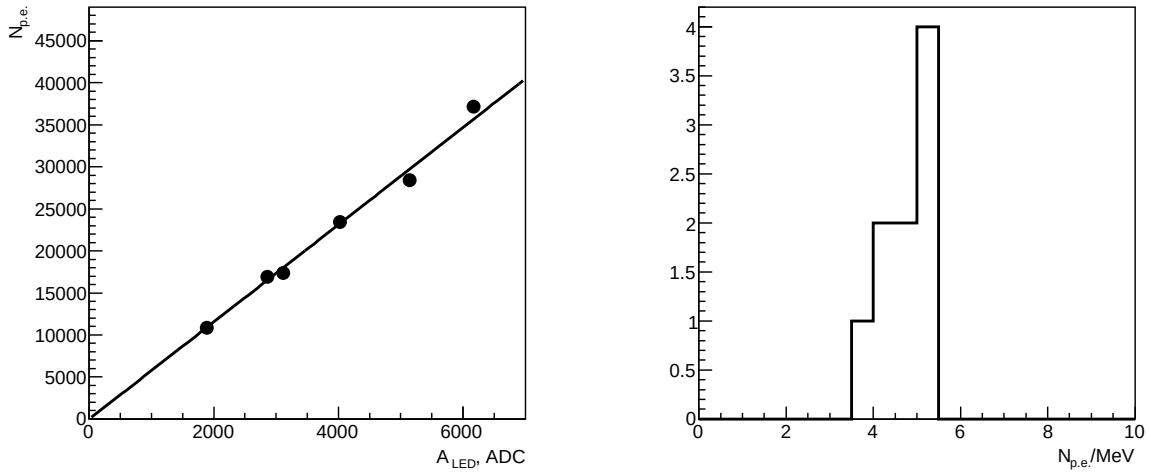

Figure 9. Light output $N_{\text{p.e.}}$ vs the LED amplitude for 1 modules (left) and the light output distribution of all 9 modules (right).

Studies were made in the electron beam energy range from 1 to 19 GeV. The energy tagged has allowed us to measure the stochastic term in energy resolution as $(2.8 \pm 0.2) \times 10^{-2}$ GeV$^{1/2}$ which is consistent with the one measured at BNL for the KOPIO project in the energy range from 0.05 GeV to 1 GeV. Taking into account the effect of light transmission in scintillator tiles and WLS fibers, photo statistics as well as noise of the entire electronic chain resulted in good agreement between the measured energy resolutions and the GEANT Monte-Carlo simulations.

The stochastic term in the dependence of position resolution on energy in our measurements is about (15.4±0.3) mm GeV$^{1/2}$ which is in agreement with Monte-Carlo simulations. For 10 GeV electrons position resolution is 6 mm in the center of the cell, and is 3 mm at a boundary between two cells.

The non-uniformity of the energy response of the prototype due to holes for straight fibers studied with the use of electrons and MIPs has turned out to be negligible. Monte-Carlo simulations are in a good agreement with the obtained experimental results.

The characteristics experimentally determined for our calorimeter prototype well meet the design goals of the PANDA and CBM experiments. However, the final conclusion on lateral sizes of the cells as well as on Shashlyk longitudinal sampling structure could be done only after studies of reconstruction efficiency of π^0-mesons of different energies.

Acknowledgment

This work was partially supported by the Rosatom grant with Ref. No. N.4d.47.03.08.118, by the INTAS grants with Ref. No. 06-1000012-8845 and 06-1000012-8914, and by the RFBR grant 05-02-08009.

References

[1] D.Alde et al. Nucl.Instr.Meth., A240(1985) 343.

[2] O.V.Buyanov et al. Nucl.Instr.Meth., A349(1994) 62.

[3] M.Beddo et al. The STAR Barrel Electromagnetic Calorimeter. Nucl. Instr .Meth. A499 (2003) 725-739

[4] "PHENIX calorimetrer", L. Aphecetche et al. NIM A499 521-536 (2003)

[5] HERA-B collaboration, HERA-B Design Report, DESY-PRC 95/01 January 1995.

[6] LHCb Calorimeters Technical Design Report, CERN/LHCC 2000-0036, September 2000.

[7] I.-H.Chiang et al. AGS Experimental Proposal 926, 1996.

[8] G.S.Atoian et al. Prepared for 11th International Conference on Calorimetry in High-Energy Physics (Calor 2004) Perugia, Italy, 28 Mar – 2 Apr 2004.

[9] G.S.Atoian et al. NIM, A 584 (2008) 291.

[10] CBM technical status report, GSI, DOC-2005-Feb-447 (2005)

[11] M.Kotulla et al. Technical Progress Report PANDA "Strong Interaction Studies with Antiprotons", February 2005.

[12] V.A.Batarin et al. Development of a Momentum Determined Electron Beam in the 1-45 GeV Range, Nucl.Instr.Meth. A510 (2003) 211–218.

[13] V.A.Batarin et al. Precision Measurement of Energy and Position Resolutions of the BTeV Electromagnetic Calorimeter Prototype, Nucl. Instrum. and Meth. **A510** (2003), 248–261.

[14] V.A.Batarin et al. LED monitoring system for the BTeV lead tungstate crystal calorimeter prototype. Nucl. Instrum. and Meth. **A534**(2004), 486–495.

[15] E.Kowalski, Nuclear Electronics. Springer, Berlin (1970).

Received October 13, 2008.

Препринт отпечатан с оригинала-макета, подготовленного авторами.

Ю.В.Харлов и др.
Свойства прототипа электромагнитного калориметра с тонким сэмплингом при энергиях от 1 до 19 ГэВ.

Оригинал-макет подготовлен с помощью системы **LaTeX.**

Подписано к печати 16.10.2008 Формат $60 \times 84/8$.
Офсетная печать. Печ.л. 1,5. Уч.-изд.л. 1,3. Тираж 90. Заказ 72.
Индекс 3649.

ГНЦ РФ Институт физики высоких энергий
142281, Протвино Московской обл.

Индекс 3649

П Р Е П Р И Н Т 2008–21, И Ф В Э, 2008